

The Impact of Thermophoresis and Brownian Motion on Non-Newtonian Fluids Flow in a Channel Due to Peristaltic Waves

Seun A. Babatunde¹, Adisa O. Areo², Olusegun A. Ajala², Henry B. Egbeyemi², Adesola D. Adediran³.

¹Department of General Studies, Federal Polytechnic, Ayede,
Ayede, Oyo State, Nigeria.

²Department of Pure and Applied Mathematics, Ladoko Akintola University of Technology,
Ogbomoso, Oyo State, Nigeria.

³Department of Mathematics and Statistics, Kwara State University,
Malete, Kwara State, Nigeria.

doi.org/10.51505/ijaemr.2026.1105

URL: <http://dx.doi.org/10.51505/ijaemr.2026.1105>

Received: Dec 03, 2025

Accepted: Dec 08, 2025

Online Published: Feb 04, 2026

Abstract

This study explores how thermophoresis and Brownian motion influence the heat and mass transfer behavior of a Casson nanofluid moving through a two-dimensional channel driven by peristaltic waves. By transforming the governing equations for momentum, energy, and nanoparticle concentration into dimensionless form and solving them numerically using the Fourth Order Runge Kutta Method (RKM4), an examination on how key parameters such as the Casson fluid parameter, Brownian motion, thermophoresis, and the Prandtl number affect velocity, temperature, and concentration profiles was carried out in this work. The findings of the analysis reveals that thermophoresis pushes nanoparticles away from heated surfaces, increasing both temperature and concentration within the channel, while Brownian motion enhances these effects through intensified particle diffusion. A higher Casson parameter reduces velocity due to greater fluid resistance, and the combined action of thermophoresis and Brownian forces strongly shapes overall heat and mass transfer. The study highlights the importance of considering non-Newtonian properties and nanoparticle dynamics when modeling peristaltic systems, with implications for thermal management, biomedical device design, and drug delivery applications.

Keywords: Thermophoresis, Brownian motion, Non-Newtonian fluid, Casson nanofluid, Peristaltic wave.

1. Introduction

Casson nanofluids have become outstandingly important because they blend the unique, non-Newtonian behavior of Casson fluids with the enhanced thermal and transport properties of nanoparticles, thereby creating materials that flow efficiently while conducting heat far better than conventional fluids. Their ability to adapt to complex flow conditions makes them valuable in a wide range of modern applications, including biomedical processes like blood-mimicking

fluids for targeted drug delivery, advanced cooling systems for electronics and renewable energy devices, industrial coating and printing technologies, and enhanced oil recovery. By improving heat transfer, reducing energy consumption, and enabling more precise control in sensitive systems, Casson nanofluids continue to play a key role in both technological innovation and practical engineering solutions [1-3].

The flow of a Casson nanofluid through a channel driven by a peristaltic wave combines the complex behavior of a yield-stress fluid with the rhythmic, wave-like motion of the channel walls. Because a Casson fluid resists deformation until a certain stress threshold is reached, the peristaltic wave plays a key role in generating enough pressure to initiate and sustain motion. As the wave propagates along the channel, it creates alternating regions of contraction and expansion that push the nanofluid forward, while the suspended nanoparticles enhance heat and mass transport. This interaction leads to distinctive velocity profiles, reduced flow reversal, and unique pressure–flow relationships that differ significantly from those of Newtonian or simple non-Newtonian fluids [4]. Javed *et al.* [5] carried out a numerical study on the peristaltic motion of Casson fluid in a channel while accounting for moderate, non-zero Reynolds numbers and magnetic field effects. Using a stream–vorticity finite-element formulation, the authors solved the governing equations and presented results through streamline and vorticity contours, velocity profiles, and pressure distributions. Their findings showed that both Reynolds and Hartmann numbers intensify flow circulation, while longitudinal velocity increases with the Casson parameter but decreases under stronger magnetic fields. The authors also compared their results with existing results in literatures and reported close agreement. Abbas *et al.* [6] examined peristaltic transport of Casson fluid in an inclined, non-uniform tube with emphasis on heat and mass transfer, including slip effects, wall properties, and the Soret and Dufour numbers. By assuming long wavelengths and low Reynolds numbers, they simplified the governing equations and derived analytical solutions, which were later validated using numerical solvers such as MATLAB's *bvp4c* and finite-element methods. Their analysis showed that increasing the Casson parameter enhances the velocity profile, while temperature rises with greater thermal slip and source/sink effects, highlighting the strong coupling between peristaltic motion and thermal transport.

Thermophoresis and Brownian motion play vital roles in shaping how Casson nanofluids behave, especially in engineering systems where heat transfer and flow control matter. Brownian motion which is the random movement of nanoparticles, tends to enhance thermal conductivity by improving microscopic mixing, which can boost the efficiency of cooling technologies like microchannel heat sinks or biomedical thermal devices. Thermophoresis, on the other hand, drives nanoparticles from hotter regions toward cooler ones, thereby influencing particle distribution and potentially altering viscosity and heat transfer rates in systems that rely on precise temperature management. In Casson fluids, which already exhibit yield-stress behavior, these particle movements can significantly affect stability, flow resistance, and overall performance, making them essential considerations in designing advanced thermal systems and smart fluid technologies [7]. Reddy *et al.*, [8] investigated how Brownian motion and

thermophoresis influence heat and mass transfer in a nanofluid flowing over a horizontal circular cylinder. Their work considered a magnetohydrodynamic (MHD) boundary layer within a porous medium and employed a robust, optimized finite element method to solve the transformed momentum, temperature, and concentration equations. The study closely examine the effect of key non-dimensional parameters, such as the magnetic parameter, thermophoresis parameter, Brownian motion parameter, tangential coordinate, and Lewis number, on the velocity, temperature, and concentration distributions. Graphical and tabulated results showed that increasing the thermophoresis parameter enlarges both thermal and concentration boundary layers, while higher Brownian motion parameter values enhance heat and mass transfer rates. On the other hand, Ramya *et al.*, [9] conducted a numerical study exploring how thermophoresis and Brownian motion affect a Casson ternary hybrid nanofluid flowing over a horizontally stretching surface populated with gyrotactic microorganisms. Their results demonstrated that thermophoresis improved fluid motion and heat transfer, whereas Brownian motion slightly reduced velocity but increased particle concentration. The numerical solutions revealed that higher microorganism density elevates the Sherwood number, indicating intensified mass transfer, while reducing concentration levels. It was also recorded in the study that increased stretching rates boosted the Nusselt number, signaling more efficient heat transport. Additionally, stronger magnetic fields raised temperature profiles but suppressed velocity, concentration, and microorganism density. Summarily, the study highlighted the superior thermal performance of Casson ternary hybrid nanofluids under these combined physical effects.

Embarking on the present study is crucial because these microscale diffusion mechanisms significantly influence heat and mass transfer behaviors in complex biological and industrial systems. Additionally, comprehending how particle migration and non-Newtonian fluid characteristics interact under peristaltic wave can improve the design and optimization of biomedical devices such as drug-delivery pumps, microfluidic systems, and artificial organs, where precise control of fluid behavior is critical. Moreover, this study aid to refine theoretical models that predict real-world transport phenomena, enabling engineers and scientists to enhance efficiency, stability, and performance in thermal management and technologies whose functionality anchors on the usage of nanofluids.

2. Mathematical Model Formulation

This study examines the peristaltic flow of a radiative Casson nanofluid within a two-dimensional channel that is filled with porous medium under the influence of magnetic field and heat source. A stationary Cartesian coordinate system (x,y) is adopted, where x -axis represents the axial direction along the channel and y -axis denotes the direction perpendicular to it as revealed in Figure 1. The channel walls, denoted by H_1 and H_2 , are maintained at constant temperatures T_0 , T_1 and, respectively. The fluid velocity components in the horizontal and vertical directions are represented by U and V . A strong transverse magnetic field of constant magnitude field strength B_0 is applied, and both Hall and Joule heating effects are incorporated into the analysis. The induced magnetic field is neglected due to the assumption of a low magnetic

Reynolds number, and the influence of an external electric field is also disregarded. Based on the formulation presented by the authors [10-11], the governing equations for the flow are expressed as follows:

Continuity equation

$$\frac{\partial U}{\partial x} + \frac{\partial V}{\partial y} = 0. \quad (1)$$

Momentum equation

$$U \frac{\partial U}{\partial x} + V \frac{\partial U}{\partial y} = \nu \left(1 + \frac{1}{\beta} \right) \frac{\partial^2 U}{\partial y^2} + U_{\infty} \frac{dU_{\infty}}{dx} - \frac{\sigma B_o^2}{\rho} (U_{\infty} - U) - \frac{\mu}{K} U. \quad (2)$$

Energy equation

$$U \frac{\partial T}{\partial x} + V \frac{\partial T}{\partial y} = \frac{\kappa}{\rho C_p} \frac{\partial^2 T}{\partial y^2} - \frac{1}{\rho C_p} \frac{\partial q_r}{\partial y} + \frac{Q_o}{\rho C_p} (T - T_{\infty}) + \frac{\nu}{C_p} \left(1 + \frac{1}{\beta} \right) \left(\frac{\partial U}{\partial y} \right)^2 + \tau \left[D_B \frac{\partial C}{\partial y} \frac{\partial T}{\partial y} + \frac{D_T}{T_{\infty}} \left(\frac{\partial T}{\partial y} \right)^2 \right]. \quad (3)$$

Concentration energy

$$U \frac{\partial C}{\partial x} + V \frac{\partial C}{\partial y} = D_B \frac{\partial^2 C}{\partial y^2} + \frac{D_T}{T_{\infty}} \frac{\partial^2 T}{\partial y^2}. \quad (4)$$

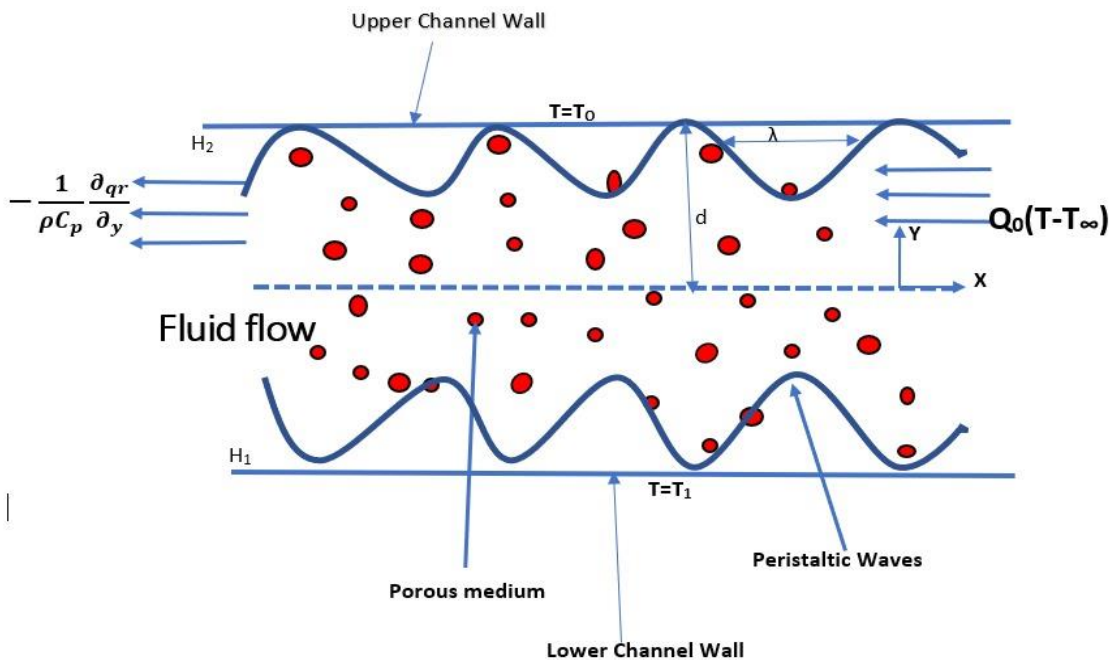


Figure 1: Schematic diagram of the problem

with the appropriate boundary conditions:

$$\text{At } y=0, u = U_w = ax^m, v = 0, -\kappa \frac{\partial T}{\partial y} = h_f(T_f - T), D_B \frac{\partial C}{\partial y} + \frac{D_T}{T_\infty} \frac{\partial T}{\partial y} = 0 \quad (5)$$

$$\text{at } y \rightarrow \infty, u = U = bx^m, T \rightarrow T_\infty, C \rightarrow C_\infty$$

Where U and V represents the dimensional velocities along the horizontal and vertical component respectively, x and y denotes the axial and normal coordinates to the channel respectively, ν is the kinematic viscosity of the fluid, β is the Casson parameter, κ is the thermal conductivity, ρ is the fluids density, C_p is the specific heat capacity at constant pressure, B_o is the magnetic field strength, σ is the electrical conductivity, q_r is the radiative heat flux, T is the fluids temperature, T_∞ is the ambient temperature, U_∞ is the ambient velocity, K is the permeability, C is the nanoparticles concentration, C_∞ is the ambient concentration, τ is the shear stress, D_B is the Brownian motion diffusion coefficient, D_T is the thermophoresis diffusion coefficient. By Rosseland approximation, the expression for the radiative heat flux according to the authors in [12] is given as,

$$q_r = \frac{-4\sigma^*}{3K^*} \left(\frac{\partial T^4}{\partial y} \right). \quad (6)$$

It is assumed that the temperature variances inside the flow are such that the term T^4 can be represented as a linear function of temperature. This is accomplished by expanding T^4 in a Taylor series about a free stream of temperature T_∞ as follows,

$$T^4 = T_\infty^4 + 4T_\infty^3(T - T_\infty) + 6T_\infty^2(T - T_\infty)^2 + \dots \quad (7)$$

Neglecting higher order terms in equation (7) beyond the first degree gives,

$$T^4 = 4T_\infty^3 T - 3T_\infty^4. \quad (8)$$

Substituting equation (8) into equation (6) gives

$$q_r = \frac{-16\sigma^* T_\infty^3}{3K^*} \left(\frac{\partial T}{\partial y} \right) \quad (9)$$

Transforming the dimensional equations in (1) – (5) via the utilization of the similarity variables and stream function in (10) gives the dimensionless momentum equation, energy equation, concentration equation with the boundary conditions as (11), (12), (13) and (14) respectively.

$$\eta = \sqrt{\frac{a}{\nu}} y, \psi = \sqrt{av} x f(\eta), \theta(\eta) = \frac{T - T_\infty}{T_w - T_\infty}, \phi(\eta) = \frac{C - C_\infty}{C_w - C_\infty}. \quad (10)$$

$$\left(1 + \frac{1}{\beta} \right) f'''(\eta) + f(\eta) f''(\eta) - (f'(\eta))^2 - M [A + f'(\eta)] + A^2 - \Gamma f'(\eta) = 0. \quad (11)$$

$$\left(1 + \frac{4}{3} N \right) \theta''(\eta) + \delta \theta(\eta) + \left(1 + \frac{1}{\beta} \right) \text{Pr Ec} (f''(\eta))^2 + \text{Pr Nb} \phi'(\eta) \theta'(\eta) + \text{Pr Nt} (\theta'(\eta))^2 + \text{Pr} f(\eta) \theta'(\eta) = 0 \quad (12)$$

$$\phi''(\eta) + \frac{N_t}{N_b} \theta''(\eta) + \text{Sc} f(\eta) \phi'(\eta) = 0. \quad (13)$$

$$\begin{aligned} \eta = 0, f(0)=0, f'(0)=A, \theta'(0)=-Bi(1-\theta(0)), Nb\phi'(0) + Nt\theta'(0)=0 \\ \eta \rightarrow \infty, f' \rightarrow 1, \theta \rightarrow 0, \phi \rightarrow 0 \end{aligned} \quad (14)$$

Where N is the radiation parameter, Γ is the porous medium parameter, M is the magnetic parameter, Bi is the Biot number, Nt is the thermophoresis parameter, Nb is the Brownian motion parameter, Sc is the Schmidt number, Pr is the Prandti number, Ec is the Eckert number, δ is the heat source parameter, and β is the Casson parameter.

3. Method of Solution

The dimensionless equations (11) to (13), subject to the boundary conditions in (14) is solved using the Runge Kutta Fourth Order Method as employed in the work of the authors [13].

Consider the initial value problem of the form.

$$\begin{aligned} y' &= f(t, y) \\ y(t_0) &= y_0 \end{aligned} \quad (15)$$

To solve equation (15) by the utilization of Runge Kutta Method Fourth Order, the formula to be employed is given as

$$y_{i+1} = y_i + \frac{h}{6}(m_1 + 2m_2 + 2m_3 + m_4). \quad (16)$$

Where

$$\begin{aligned} m_1 &= hf(t_i, y_i) \\ m_2 &= hf\left(t_i + \frac{h}{2}, y_i + \frac{m_1}{2}\right) \\ m_3 &= hf\left(t_i + \frac{h}{2}, y_i + \frac{m_2}{2}\right) \\ m_4 &= hf(t_i + h, y_i + m_3) \end{aligned} \quad (17)$$

Where h is the step length?

4. Discussion of Results

In this study, we present graphically and discuss extensively the influence of varying flow parameters on velocity, temperature and concentration profile.

Enhancing the Schmidt number $Sc=0.1,0.3,0.5,0.7$ results to a decline in the velocity of the fluid as revealed in Figure 2. A rise in the Schmidt number, which represents the ratio of momentum diffusivity to mass diffusivity, means that the fluid's momentum diffuses more quickly relative to mass diffusion. For a Casson nanofluid which is a non-Newtonian fluid with

yield stress and suspended nanoparticles, an increase in Schmidt number tends to reduce the velocity because the fluid resists changes in concentration more strongly, leading to a thicker concentration boundary layer and enhanced viscous effects. This results in slower fluid motion as momentum transfer dominates over mass transfer. From an engineering perspective, understanding this behavior is crucial when designing systems like heat exchangers, biomedical devices, or industrial mixers where precise control over flow and mass transfer is required, ensuring efficiency and performance are maintained despite changes in fluid properties. Figure 3 demonstrates that raising the Eckert number $Ec=0.2,0.4,0.6,0.8$ results into an enhancement in the velocity of the fluid. An increase in the Eckert number, which represents the ratio of kinetic energy to enthalpy difference, typically leads to a rise in the velocity of a Casson nanofluid. This happens because higher Eckert numbers indicate stronger viscous dissipation, which in turn generates more thermal energy within the fluid. In a Casson fluid, which behaves like a shear-thinning fluid with a yield stress, this added thermal energy reduces the fluid’s effective viscosity, making it easier to flow and thus increasing its velocity. From an engineering perspective, this has important implications in systems like microfluidic devices or thermal management in

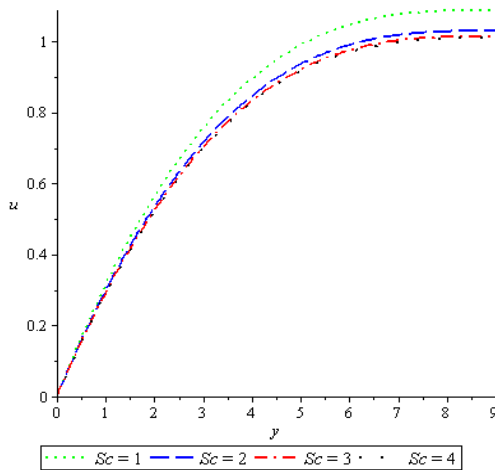


Fig. 2. Effect of Sc on velocity profile

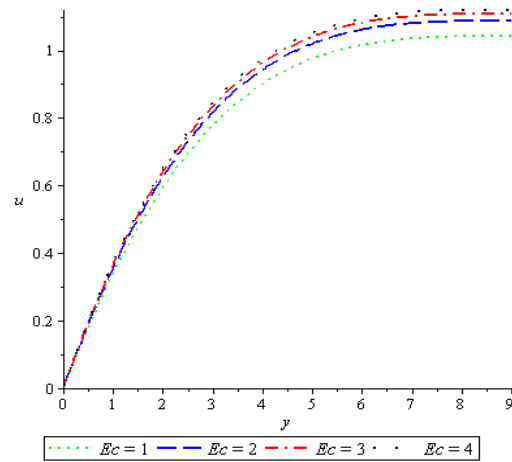


Fig. 3. Effect of Ec on velocity profile

electronics, where precise control of fluid flow and heat transfer is critical. By managing the Eckert number, engineers can optimize fluid speed and thermal behavior to enhance efficiency and performance.

Figure 4 demonstrates that a rise in Prandtl number $Pr=0.1,0.3,0.5,0.7$ causes a decline in the velocity of the fluid. A rise in the Prandtl number, which represents the ratio of momentum diffusivity to thermal diffusivity, generally leads to a decrease in the velocity of a Casson nanofluid. This occurs because higher Prandtl numbers indicate lower thermal conductivity,

causing the fluid to retain heat more effectively and reduce the rate of thermal diffusion. As a result, the fluid becomes more resistant to flow under thermal gradients, slowing its motion. In engineering applications, this behavior is significant in thermal insulation systems or processes where controlling the rate of heat transfer is essential, such as in polymer processing or thermal barrier coatings, where slower-moving fluids help maintain temperature stability. Figure 5 shows that increasing the Brownian motion parameter $Nb=0.2, 0.4, 0.6, 0.8$ causes a jump in the

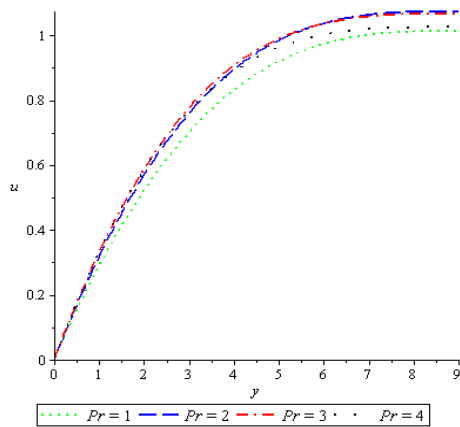


Fig. 4. Effect of Pr on velocity profile

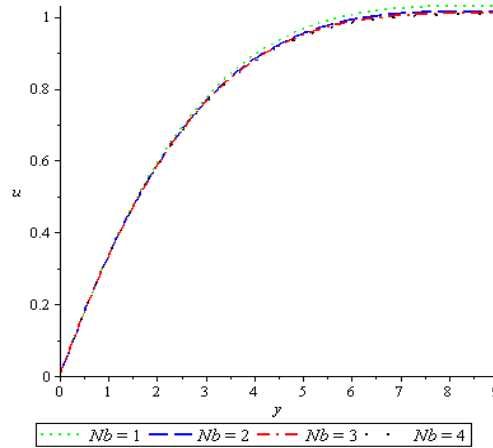


Fig. 5. Effect of Nb on velocity profile

velocity of the fluid. An increase in the Brownian motion parameter enhances the random movement of nanoparticles within a Casson nanofluid, which leads to greater momentum transfer at the microscopic level. This typically results in an increase in the overall velocity of the nanofluid, as the enhanced particle diffusion reduces viscous resistance and promotes fluid mixing. From an engineering perspective, this implies improved thermal and fluid transport characteristics, which can be advantageous in applications like microfluidic cooling systems, drug delivery, and energy systems where efficient heat and mass transfer are critical. A rise in radiation parameter $N=0.3, 0.6, 0.9, 1.2$ leads to a rise in the velocity of the fluid flowing in the channel as demonstrated in figure 6. An increase in the radiation parameter typically leads to a rise in the velocity of a Casson nanofluid. This is because higher thermal radiation enhances the thermal energy within the fluid, reducing its viscosity and promoting greater molecular motion, which in turn facilitates faster flow. In engineering, this effect is particularly important in thermal management systems, such as in cooling technologies for electronic devices or in solar energy collectors. By understanding how radiation influences temperature is critical. Figure 7 shows that an increase in thermophoresis parameter $Nt=0.2, 0.4, 0.6, 0.8$ results to a decline in the fluid's velocity. An increase in the thermophoresis parameter in a Casson nanofluid typically leads to a decrease in the fluid's velocity. Thermophoresis refers to the movement of nanoparticles from hotter to cooler regions, driven by temperature gradients. As this effect intensifies, more nanoparticles migrate away from the heated surface, causing an accumulation in

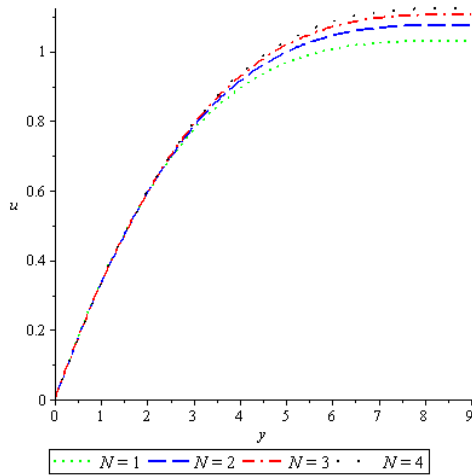


Fig. 6. Effect of N on velocity profile

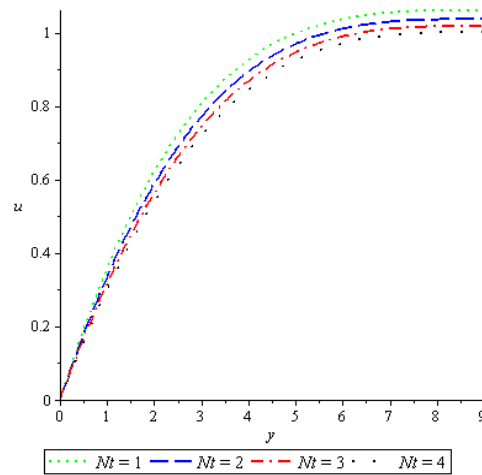
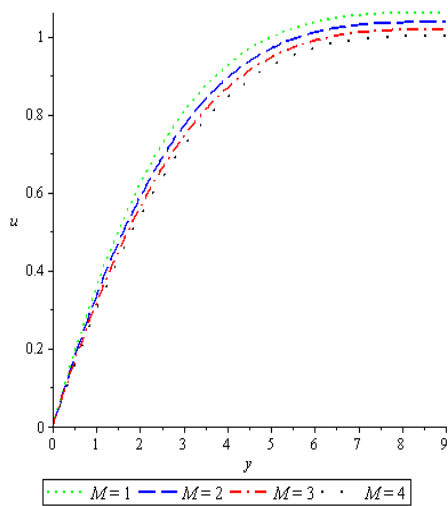
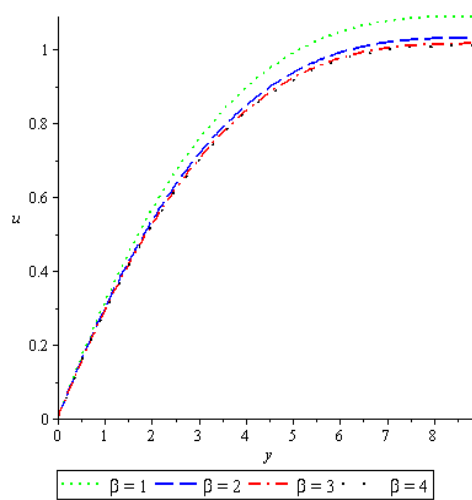


Fig. 7. Effect of Nt on velocity profile

cooler regions. This redistribution alters the local viscosity and thermal conductivity, often thickening the boundary layer and increasing resistance to flow, thus reducing velocity. From an engineering perspective, this has important implications in thermal management systems, such as in cooling of electronic devices or in biomedical applications, where precise control of heat and nanoparticle distribution is critical for maintaining efficiency and preventing overheating. Figure 8 shows that a rise in magnetic parameter $M = 0, 0.25, 0.5, 0.75$ leads to a decline in the velocity of the fluid. An increase in the magnetic parameter (often referred to as the Hartmann number) generally leads to a decrease in the velocity of a Casson nanofluid flowing through a channel. This occurs because the magnetic field introduces a Lorentz force that acts in opposition to the fluid motion, effectively damping the flow and increasing resistance. The stronger the magnetic field, the greater this resistive force, resulting in slower fluid movement. This effect is particularly relevant in electrically conducting fluids, where magnetic control is used to regulate flow characteristics. One practical engineering application of this phenomenon is in the cooling systems of nuclear reactors, where magnetohydrodynamic (MHD) control is used to manage the flow of nanofluids that serve as efficient coolants, ensuring safe and stable reactor operation. An increase in Casson parameter $\beta = 0.5, 1.0, 1.5, 2.0$ reduces the velocity of the fluid as shown in Figure 9. An increase in the Casson parameter, which characterizes the fluid's yield stress behavior, leads to a decrease in the velocity of a Casson nanofluid. Physically, a higher Casson

Fig. 8. Effect of M on velocity profileFig. 9. Effect of β on velocity profile

parameter indicates that the fluid behaves more like a solid and requires greater force to initiate flow. As this parameter rises, the fluid's resistance to deformation increases, resulting in a thicker momentum boundary layer and reduced flow velocity. In engineering applications, this behavior is especially relevant in industries involving non-Newtonian fluids such as blood analogs, paints, or polymer solutions. For example, in biomedical engineering, understanding how blood flow (which behaves like a Casson fluid) slows down under certain conditions can aid in designing medical devices like stents or artificial heart valves to ensure optimal flow and minimize risks of clotting. Figure 10 reveals that a rise in radiation parameter $N=0.3, 0.6, 0.9, 1.2$ leads to a rise in the temperature of the Casson nanofluid. An increase in the thermal radiation parameter enhances the temperature of a Casson nanofluid because it intensifies the radiative heat flux within the fluid. As radiation becomes more significant, it acts as an additional mode of heat transfer, raising the overall thermal energy distributed throughout the fluid. This effect is especially pronounced in nanofluids, which already possess high thermal conductivity due to the presence of nanoparticles. From an engineering perspective, this can be advantageous in applications like thermal energy storage systems or high-efficiency cooling in electronics, where maintaining elevated and uniform temperatures improves performance. However, it may also necessitate improved thermal management to prevent overheating in sensitive components.

Figure 11 reveals that an enhancement in the Eckert number $Ec=0.2, 0.4, 0.6, 0.8$ resulted into an enhancement in the temperature of the Casson nanofluid. As the Eckert number rises, it indicates that the kinetic energy of the fluid flow is being converted into internal energy, which increases the temperature of the Casson nanofluid. This happens because higher viscous dissipation generates more heat within the fluid, raising its thermal energy. From an engineering perspective, this means that in applications involving high-speed or high-viscosity flows of Casson nanofluids—like in cooling systems or lubricants—engineers must carefully manage the heat buildup to avoid overheating, which could affect performance or cause material degradation.

Proper design might involve enhanced cooling strategies or selecting nanofluid compositions that handle the extra thermal load efficiently. Figure 12 shows that a rise in magnetic parameter $M = 0, 0.25, 0.5, 0.75$ leads to a rise in the temperature of the Casson nanofluid. An increase in the magnetic parameter, which represents the influence of an applied magnetic field, typically leads to a rise in the temperature of a Casson nanofluid due to enhanced resistive (Joule) heating. The magnetic field creates a Lorentz force that opposes fluid motion, increasing viscous dissipation and converting more kinetic energy into thermal energy. This elevates the fluid's temperature, particularly near the boundary layer. From an engineering perspective, this behavior is crucial in applications like thermal management in electronic systems or magnetohydrodynamic (MHD) pumps, where precise temperature control is essential. Understanding this effect allows engineers to fine-tune magnetic fields to optimize heat transfer or maintain operational safety in systems utilizing non-Newtonian nanofluids. An increase in Casson parameter $\beta = 0.5, 1.0, 1.5, 2.0$ increases the temperature of the Casson fluid, as shown in Figure 13. An increase in the Casson parameter indicates a stronger yield stress in the nanofluid, meaning the fluid resists flow more significantly before it starts moving. This increased resistance slows down the fluid motion, reducing the overall convective heat transfer within the system. As a result, the temperature of the Casson nanofluid tends to rise, especially in regions close to heat sources. From an engineering standpoint, this behavior implies that systems relying on efficient cooling—such as microfluidic devices, biomedical instruments, or heat exchangers—may experience overheating if the Casson parameter is too high. Engineers must therefore carefully consider fluid properties during system design to ensure adequate thermal regulation. Figure 14 revealed that an increase in Brownian motion parameter $Nb = 0.2, 0.4, 0.6, 0.8$ increases the temperature of the Casson nanofluid. An increase in the

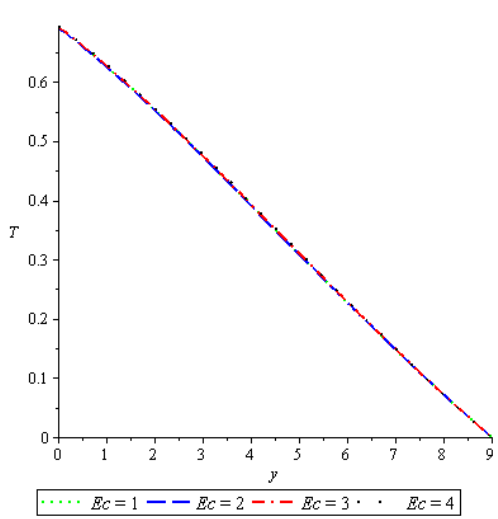


Fig. 11. Effect of Ec on temperature profile

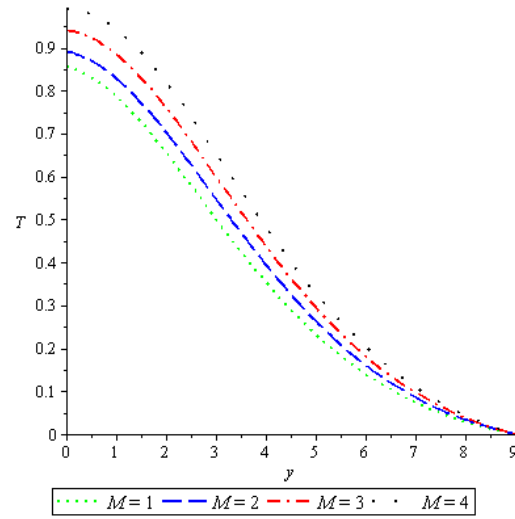
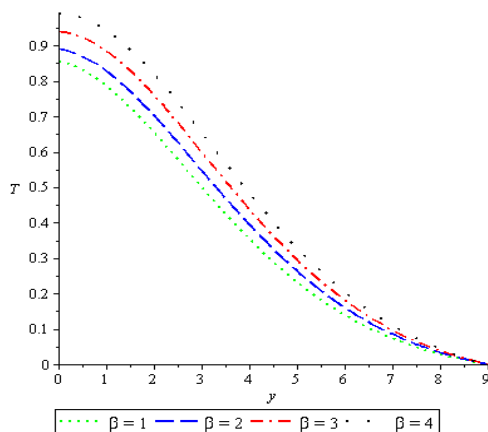
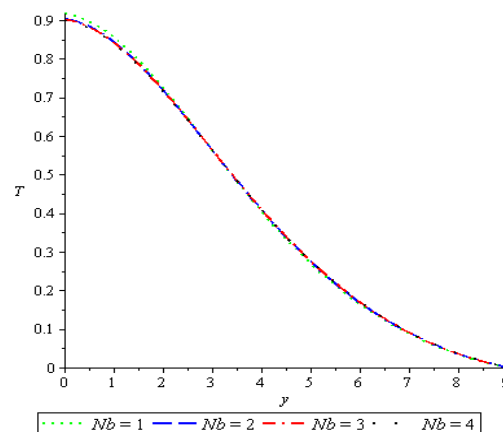


Fig. 12. Effect of M on temperature profile

Fig. 13. Effect of β on temperature profileFig. 14. Effect of Nb on temperature profile

Brownian motion parameter in a Casson nanofluid generally leads to enhanced random movement of nanoparticles, which boosts the thermal energy distribution within the fluid, effectively raising its temperature. This is because the intensified Brownian motion facilitates better heat transfer at the microscopic level by increasing the interaction and collision rates among particles, thus improving the fluid's thermal conductivity. From an engineering perspective, this implies that controlling the Brownian motion parameter—through nanoparticle size, concentration, or fluid viscosity—can be a strategic way to optimize the heat transfer performance in systems like cooling devices or heat exchangers that use Casson nanofluids, enabling more efficient thermal management in industrial applications. Figure 15 demonstrated that a rise in Prandtl number $Pr=0.1, 0.3, 0.5, 0.7$ causes a rise in the temperature of the fluid. When the Prandtl number rises in a Casson nanofluid, it means the fluid's momentum diffusivity increases relative to its thermal diffusivity, which tends to slow down heat transfer through the fluid. As a result, the temperature within the nanofluid can become higher because heat spreads more slowly, causing the fluid to retain heat longer. For engineers, this means that adjusting the Prandtl number—by changing the fluid's properties or operating conditions—can help control how heat is distributed and maintained in systems like cooling channels or microfluidic devices. Managing this balance is crucial for designing efficient thermal systems where precise temperature control is needed, such as in electronics cooling or biomedical applications. An enhancement in the Schmidt number $Sc=0.1, 0.3, 0.5, 0.7$ leads to a decline in the temperature of the Casson nanofluid, as revealed in Figure 16. An increase in the Schmidt number, which represents the ratio of momentum diffusivity (viscosity) to mass diffusivity, means that the mass diffusion of nanoparticles or solutes in the Casson nanofluid becomes slower compared to momentum transfer. This leads to a thinner concentration boundary layer and less nanoparticle movement, which in turn reduces the effectiveness of nanoparticle-driven thermal conductivity enhancement. As a result, the overall temperature of the fluid may decrease slightly due to reduced convective heat transfer. From an engineering standpoint, this suggests that in systems relying on nanofluids for improved thermal performance—such as microchannel heat sinks or

biomedical cooling devices—operating at high Schmidt numbers might limit the intended heat transfer benefits, necessitating careful selection of fluid properties to maintain thermal efficiency. Figure 17 shows that an increase in thermophoresis parameter $Nt=0.2, 0.4, 0.6, 0.8$ results to a rise in the Casson nanofluids temperature. An increase in the thermophoresis parameter in a

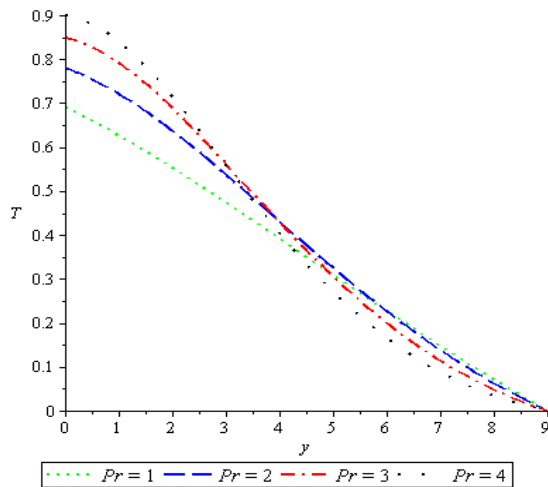


Fig. 15. Effect of Pr on temperature profile

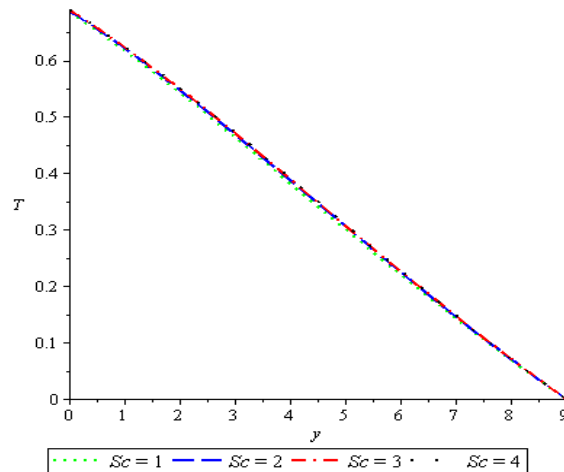


Fig. 16. Effect of Sc on temperature profile

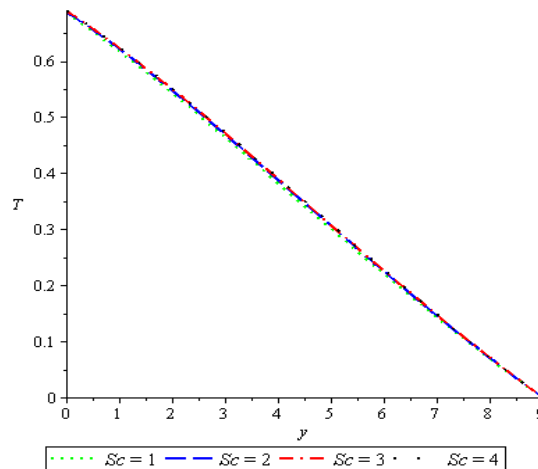


Fig. 17. Effect of Nt on temperature profile

system where Casson nanofluids flow generally leads to a rise in fluid temperature. Thermophoresis refers to the movement of nanoparticles from hot regions to cooler ones, and a higher thermophoresis parameter intensifies this motion. As nanoparticles migrate, they carry heat with them, altering the local thermal gradients and often resulting in a thicker thermal boundary layer and reduced heat dissipation. This can raise the overall temperature within the

system. From an engineering perspective, this effect is crucial in applications like microelectronic cooling or biomedical thermal therapies, where precise thermal control is needed. If not managed properly, increased thermophoretic effects could lead to hotspots and reduced cooling efficiency, requiring enhanced design strategies for thermal regulation. Figure 18 reveals that a rise in Casson parameter $\beta=0.5,1.0,1.5,2.0$ leads to a decline in the concentration profile. An increase in the Casson parameter, which characterizes the yield stress behavior of a Casson nanofluid, generally leads to a decrease in the fluid's velocity and enhances its resistance to flow. As the Casson parameter rises, the fluid behaves more like a solid until a certain stress threshold is overcome, which causes a suppression in the convective transport of nanoparticles. This reduction in movement limits the dispersion and mixing of nanoparticles, resulting in a lower concentration of nanofluid in the flow field. From an engineering perspective, this implies that systems relying on effective heat transfer or mixing, such as cooling devices or biomedical flows, may experience reduced efficiency when the Casson parameter is high. Therefore, understanding and controlling this parameter is crucial in designing systems that require precise thermal management or consistent nanoparticle distribution. Figure 19 shows that a rise in magnetic parameter $M=0,0.25,0.5,0.75$ leads to a decline in concentration profile. An increase in the magnetic parameter generally leads to a suppression of the concentration profile in a Casson nanofluid. This happens because a stronger magnetic field induces a Lorentz force that acts opposite to the fluid motion, effectively slowing down the flow. As the flow decelerates, the transport of nanoparticles due to convection is reduced, leading to a thinner concentration boundary layer. Consequently, the nanoparticle concentration near the surface diminishes, resulting in a lower overall concentration profile across the fluid domain. This behavior is particularly significant in electrically conducting fluids where magnetic effects are pronounced. Figure 20 demonstrates that increasing the Brownian motion parameter $Nb=0.2,0.4,0.6,0.8$ causes a decline in the concentration of the nanoparticles. An increase in the Brownian motion parameter in a Casson nanofluid enhances the random movement of nanoparticles, causing them to spread more uniformly throughout the fluid. This increased diffusion tends to reduce the concentration gradient near the surface, leading to a slight decrease in nanoparticle concentration at the boundary layer. From an engineering perspective, this effect can impact the design of nanofluid-based systems such as biomedical devices or microfluidic channels, where precise control of nanoparticle distribution is critical for drug delivery efficiency or thermal regulation at

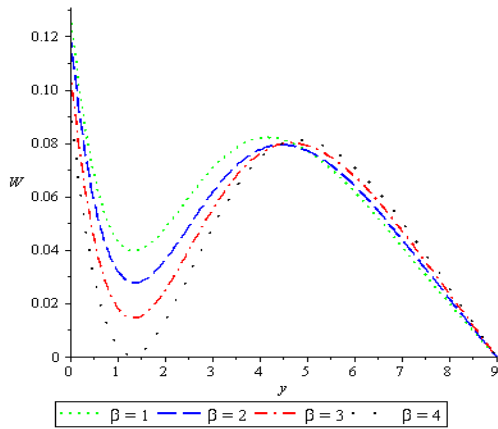


Fig. 18. Effect of β on concentration profile

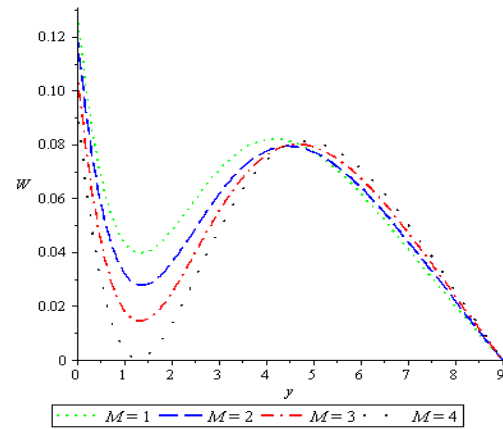


Fig. 19. Effect of M on concentration profile

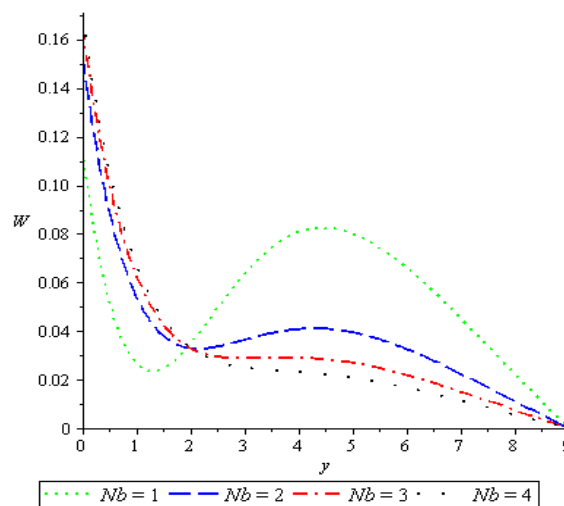


Fig. 20. Effect of Nb on concentration profile

the microscale. Increasing the thermophoresis parameter $Nt=0.2,0.4,0.6,0.8$ leads to an enhancement of the nanoparticles concentration, as revealed in

Figure 21. An increase in the thermophoresis parameter in a Casson nanofluid flow leads to a higher migration of nanoparticles from hotter to cooler regions, which enhances the nanoparticle concentration away from the heated surface. This occurs because thermophoresis drives particles along temperature gradients, and a stronger parameter intensifies this effect. From an engineering standpoint, this behavior can be utilized to improve the efficiency of thermal management systems, such as in electronic cooling or heat exchangers, by optimizing nanoparticle distribution to enhance thermal conductivity in targeted areas, thereby improving heat dissipation and overall

system performance. Figure 22 unfolds that an enhancement in Eckert number $Ec=0.2,0.4,0.6,0.8$ causes a decline in the Casson nanofluids concentration. An enhancement in the Eckert number, which measures the ratio of kinetic energy to enthalpy (essentially capturing the effect of viscous dissipation), leads to more internal heat generation within the Casson nanofluid due to frictional heating. This added thermal energy raises the fluid temperature, enhancing Brownian motion and thermophoretic forces, which in turn causes nanoparticles to disperse more and reduces their concentration near the surface. In engineering applications, this can be beneficial for processes requiring uniform nanoparticle distribution, such as in cooling systems or material processing. However, excessive viscous heating might reduce thermal efficiency or damage temperature-sensitive components, requiring careful design considerations. A rise in the Schmidt number $Sc=0.1,0.3,0.5,0.7$ causes a decline in the concentration profile as revealed in Figure 23. An increase in the Schmidt number (Sc), which represents the ratio of momentum diffusivity to mass diffusivity, leads to a decrease in the concentration boundary layer thickness of a Casson nanofluid. This means that as Sc increases, mass diffusion becomes slower compared to momentum diffusion, resulting in a lower concentration of nanoparticles near the surface. In industrial and engineering applications, such as in drug delivery, cooling of electronic devices, or chemical processing, this behavior is significant because it affects the efficiency of mass transfer processes. For instance, lower nanoparticle concentration near surfaces might reduce the effectiveness of thermal conductivity enhancement or chemical reaction rates, necessitating adjustments in system design or operating conditions to maintain performance. Enhancing radiation parameter $N=0.3,0.6,0.9,1.2$ decreases the concentration profile, as shown in Figure 24. An increase in the thermal radiation parameter generally enhances the thermal energy within the fluid, leading to a rise in temperature, which, in turn, reduces the fluid's viscosity and alters the nanoparticle concentration distribution.

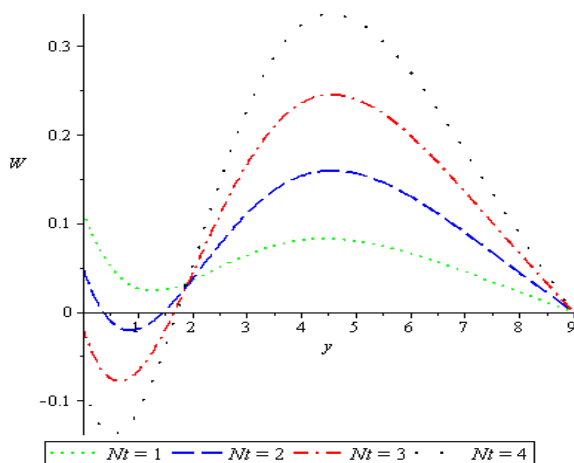


Fig. 21. Effect of Nt on concentration profile

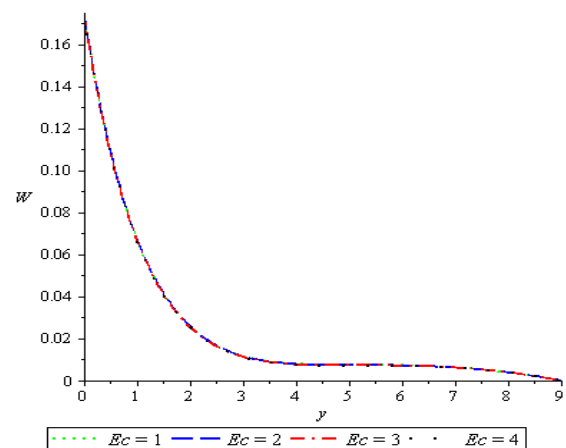


Fig. 22. Effect of Ec on concentration profile

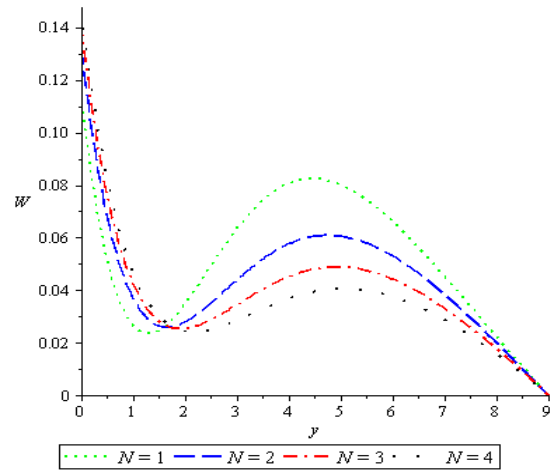
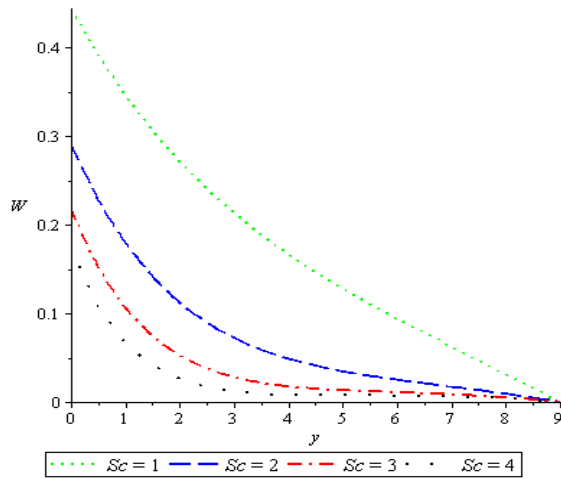


Fig. 23. Effect of Sc on concentration profile

Fig. 24. Effect of N on concentration profile

In the context of a Casson nanofluid, which exhibits non-Newtonian behavior, higher thermal radiation causes increased Brownian motion and thermophoretic diffusion of nanoparticles. This typically leads to a decrease in nanoparticle concentration near the heated surface due to stronger thermophoretic forces pushing particles away from high-temperature regions. Industrially, this behavior is crucial in applications such as thermal management systems, polymer processing, and nano-coating technologies, where precise control of particle dispersion and heat transfer is essential for optimizing performance, ensuring uniform product quality, and preventing clogging or sedimentation in microfluidic systems. An enhancement in the Prandtl number $Pr=0.1, 0.3, 0.5, 0.7$ leads to a rise in the concentration of Casson nanofluid as revealed in Figure 25. Increasing the Prandtl number, which represents the ratio of momentum diffusivity to thermal diffusivity, generally leads to a thicker momentum boundary layer and a thinner thermal boundary layer. In the context of Casson nanofluids (non-Newtonian fluids with yield stress behavior), this results in reduced thermal diffusion and enhanced resistance to heat penetration. Consequently, the concentration of nanoparticles tends to increase near the surface due to weaker thermal gradients and slower diffusion rates. From an engineering standpoint, this implies improved thermal insulation characteristics but could also lead to aggregation or clogging issues in microfluidic or heat transfer systems, especially where precise control of nanoparticle distribution is critical.

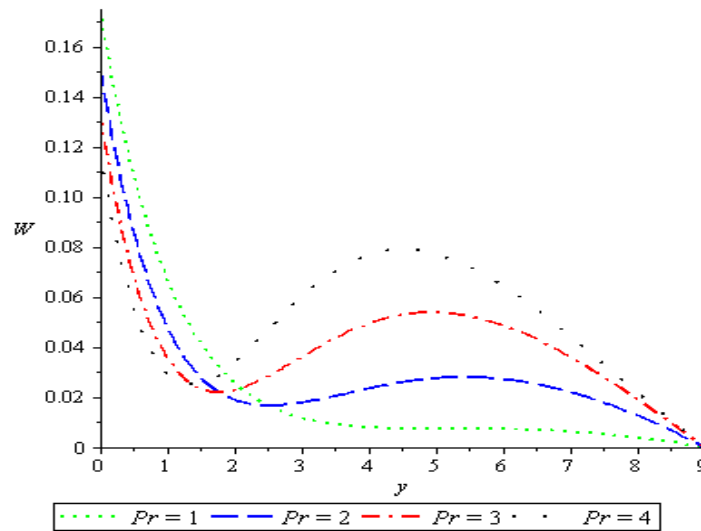


Fig. 25. Effect of Pr on concentration profile

5. Conclusion and Recommendation

A new mathematical model was developed to describe how a non-Newtonian Casson nanofluid moves through a channel under the influence of a peristaltic wave. The model incorporates the combined effects of thermophoresis and Brownian motion, which influence how nanoparticles distribute within the fluid. After formulating the governing equations, the study applied a non-dimensionalisation process using appropriate similarity variables to simplify the system. The resulting dimensionless equations were solved numerically using the fourth-order Runge–Kutta method. The study also explored how various physical parameters—such as magnetic field strength, thermal radiation, Casson fluid characteristics, thermophoresis and Brownian motion effects, Prandtl number, Eckert number, and Schmidt number—impact the fluid's velocity, temperature, and concentration profiles. These effects were illustrated through graphical results and interpreted in terms of their physical significance.

Based on the outcomes of this research, it is therefore recommended that engineers in the field of design and maintenance should take into consideration parameters that influence the fluid flow, the temperature within the system and also the concentration of the nanoparticles when designing engineering and technological devices whose functionality anchors on the usage of Casson nanofluid. Utilising this information will ensure better performance and high reliability of systems, while failure to adhere to the aforementioned informations may lead to optimum ineffectiveness of the devices.

References

- Choi, S.U.S. Enhancing thermal conductivity of fluids with nanoparticles. *ASME Publ. Fed.* **1995**, 231, 99–106.
- Xuan, Y.; Li, Q. Investigation on convective heat transfer and flow features of nanofluids. *J. Heat Transf.* **2003**, 125, 151–155.
- Khalili, S.; Tamim, H.; Khalili, A.; Rashidi, M.M. Unsteady convective heat and mass transfer in pseudoplastic nanofluid over a stretching wall. *Adv. Powder Technol.* **2015**, 26, 1319–1326.
- Deepalakshmi, P. Shyq, R., Loganathan, K. Two-phase MHD peristaltic flow of non-Newtonian Casson fluid through through the renal tube in the presence of microliths. *ThermoFluids*, 4(4), 406-447, (2024).
- Jayed, T., Ahmed, B., Hamid, A. H., Sajia, M.. Numerical analysis of peristaltic transport of Casson fluid for non-Zero Reynolds number in the presence of the magnetic field. *ThermoFluids*, 2(11), 10-30, 2018.
- Abbas, Z., Rafiq, Y., Jayed, T. (2020). Peristaltic transport of a Casson fluid in a non-uniform tube with Rosseland approximation and wall properties. *Mathematical Engineering*, 6, 1997-2007.
- Vaidya, H., Mebarek, K., Kumar, R. Magnetohydrodynamic peristaltic propulsion of Casson nanofluids with slip effects over heterogenous rough channel. *Applied Mathematics*, 2(11), 3-21, 2024.
- Reddy, R. O., Reddy, S., Reddy, O., Chamkha, A. J. Effect of Brownian motion and thermophoresis on heat and mass transfer flow over a horizontal circular cylinder filled with nanofluid. *Journal of Nanofluids*, 6, 702-710, 2017.
- Ramya, P., Deivanayaki, M., Pandurengan, S. Thermophoresis and Brownian motion effects on the Casson ternary hybrid nanofluid over a horizontal plate containing gyrotactic microorganisms. *Mathematical Engineering*, 6(2), 344-360, 2024.
- Hani, U., Ali, M., Alam, M. S. Magnetohydrodynamic mixed convection heat and mass transfer of nanofluid flow over a stretching wedge-shaped surface with the effect of thermophoresis and Brownian motion. *Journal of Nanofluids*. 12, 1600-1664, 2023.
- Ajala, A., Ogundiran, S. D., Salawu, S. O. Unsteady mixed convective flow of Casson nanofluid in a Darcy-Forchheimer medium with slip and temperature jump condition. *International Journal of Innovative Science and Research Technology*, 9(1), 2024.
- Oderinu, R. A., Salawu, S. O., Ohaegbue, A. D., Alao, S., Sulaiman, N. G. Computational study of thermal criticality and irreversibility of a double exothermic hydromagnetic fluid in a vertically positioned porous channel. *Thermal Advances*, **25**, 101039, 2025.
- Nawaz, Y., Majeed, A. H., Waheed, H. A. Stability and convergence analysis for coupling of exponential integrator and Runge Kutta method for Eyring-Powell fluid under unsteady Electro-Osmosis flow effects. *Ricerche di Matematica*, 2025.
- Xinchao, W., Ting, F., Wang, J., Zeng, L., Zhang, F. A comparative study of fluid flow and heat transfer in the tube with multi-v-winglets vortex generators. *Applied Thermal Engineering*. **236**(32), 121-130, 2024.

- Xue, P., Si, X., Ding, W., Li, C., Oi, J., Cao, J. Investigating the role of surface contact area adjustment for enhancing interfacial heat transfer of the Cf/C-Havnes 230 joint. *Materials Characterization*. **215**(21), 112-120, 2024.
- Yuqi, S., Zhao, Y., Zijian, L., Flammability inhibition effect assessment with mildly flammable refrigerant and inert gases on difluoromethane. *International Journal of Refrigeration*. **144**(2), 26-33, 2022.
- Zafar, M., Sidra, J., Fuad, A., Emad, A. A. Investigation of entropy generation in the existence of heat generation and nanoparticle clustering on porous riga plate during nanofluid flow. *Materials Today Communications*. **38**(10), 108-120, 2024.
- Zhao, X., Rui, X., Wang, Y., Zhang, R. A novel method for prediction of propellant shell-life based on Arrhenius equation. *Propellants, Explosives, Pyrotechnics*, **43**(4), **348-354**, **2018**.
- Zhenye, L., Yue, H., Ralf, D., Han, P., Yancheng, Y. Flow characterization during the flame acceleration and transition-to-detonation process with solid obstacles and fluid jets. *Shock Waves*. **32**(7), 617-632, 2022.
- Sharma, P., Saboo, R., Chaudhary, R. Radiative and chemically reactive MHD fluid flow through a two-region heated vertical channel with heat and mass transfer. *AIP Conference Proceedings*, **3025**(1), **2024**.
- Shen, N., Liao, J., Bal, S., Li, S. Systematic construction of combustion reaction in model for large hydrocarbon fuels based on a two-step reaction scheme. *Combustion and Flame*. **260**(10), 113-120, 2024.